

POLARISED HIGH- Q^2 DEEP INELASTIC SCATTERING AT HERA-II

K. NAGANO

ON BEHALF OF THE H1 AND ZEUS COLLABORATIONS

*DESY c/o F1J, Notkestrasse 85, 22603 Hamburg, Germany**E-mail: nagano@mail.desy.de*

The cross sections for neutral and charged-current deep inelastic scattering with longitudinally polarised e^+p collisions were first measured at a luminosity-averaged positive polarisation of about 30% and at a negative polarisation of about -40%. The parity-violating nature of the weak charged-current interaction was clearly observed, which is the first direct measurement at large energies.

1 Deep inelastic scattering at HERA

Deep inelastic scattering (DIS) of leptons off nuclei has been the key to our understanding of the structure of the nucleon. HERA at DESY is the sole facility which collides electrons or positrons (e^\pm) with protons (p). Owing to the large centre-of-mass energy of about 320 GeV, the kinematic region to explore the p structure has been significantly extended by HERA. The two collider experiments, H1 and ZEUS, collected about 100 (20) pb^{-1} of luminosity for unpolarised collisions of e^+ (e^-) and p up until the year 2000 (HERA-I). Precise measurements of DIS cross-sections and hence of the p structure functions were made, which have led to new insights and precise knowledge of the p structure^{1,2}. For example, the DGLAP-evolution based perturbative QCD (pQCD) was found to give an excellent description over such a wide kinematic range as 5 orders of magnitude in the four-momentum transfer squared (Q^2). The parton distribution functions (PDFs) of gluon and sea quarks were precisely determined in the small Bjorken- x region^{3,4}.

After the year 2000, HERA underwent a major upgrade (HERA-II) aiming for higher luminosity and for collisions with longitudinally polarised e^\pm . The higher luminosity will give sensitivity in the largest Q^2 region where the electro-weak (EW) interaction

dominates, and the longitudinal polarisation of the e^\pm beam will give a direct sensitivity to the helicity structure of the EW interaction. HERA-II data-taking was resumed from autumn 2003 with remarkable success in improving background conditions in the experiments, and both HERA and the experiments attained stable and high-efficiency operation. The H1 (ZEUS) collaboration has collected 15.3 (14.1) pb^{-1} of e^+p collisions at luminosity-averaged e^+ polarisation of +33.0 (+31.8) % and 21.7 (16.4) pb^{-1} at luminosity-averaged e^+ polarisation of -40.2 (-40.2) %^a. Based on these data samples, the first measurement of longitudinally polarised e^+p high- Q^2 DIS cross-sections was made, and is reported in this manuscript^{5,6}.

2 Longitudinally polarised $e^\pm p$ DIS

The charged-current (CC) DIS interaction, $e^{+(-)}p \rightarrow \bar{\nu}(\nu)X$, is a purely weak interaction. Therefore, as a direct consequence of the Standard Model (SM)'s fully parity-violating nature of the weak charged-current interaction, the cross-section depends on the longitudinal polarisation of e^\pm , P , as:

$$\sigma_{CC}^{P,\pm} = (1 \pm P)\sigma_{CC}^{0,\pm},$$

where $\sigma_{CC}^{0,\pm}$ denotes the cross-section for unpolarised $e^\pm p$ DIS. Polarisation is defined as $P = \frac{N_R - N_L}{N_R + N_L}$, where N_R (N_L) denotes the number of right-handed (left-handed) e^\pm .

^aFor the definition of polarisation, refer Sect. 2.

The neutral-current (NC) DIS interaction, $e^\pm p \rightarrow e^\pm X$, is mediated by γ and Z . Therefore, the cross-section dependence on longitudinal polarisation of e^\pm is given by the pure Z -exchange and interference between γ and Z , and hence becomes prominent only at large Q^2 . The cross-section can be written as ^b:

$$\tilde{\sigma}_{NC}^\pm = Y_+[F_2^{0,\pm} + PF_2^{P,\pm}] + Y_-[xF_3^{0,\pm} + PxF_3^{P,\pm}],$$

where the reduced cross-section $\tilde{\sigma}_{NC}^\pm$ is defined as $(d^2\sigma_{NC}^\pm/dxdQ^2)/(2\pi\alpha^2Y_\pm/xQ^4)$, α is the electromagnetic fine structure constant and $Y_\pm = 1 \pm (1-y)^2$, with y being the inelasticity ⁸. The structure functions F_2^0 and xF_3^0 are for unpolarised $e^\pm p$, and the polarised structure functions are defined as:

$$\begin{aligned} F_2^{P,\pm} &= \sum x(q + \bar{q})[\mp 2aQ_q v_q K_Z \\ &\quad \pm 2va(v_q^2 + a_q^2)K_Z^2], \\ xF_3^{P,\pm} &= \sum x(q - \bar{q})[2vQ_q a_q K_Z \\ &\quad - 2(v^2 + a^2)v_q a_q K_Z^2], \end{aligned}$$

where the sum runs over quark flavours, and Q_q is the charge, a_q and v_q are the axial and vector couplings of the quark q . The kinematic factor K_Z is defined as $K_Z = \frac{Q^2}{Q^2 + M_Z^2} \frac{1}{4\sin^2\theta_W \cos^2\theta_W}$ with θ_W being the Weinberg angle, and a and v are the axial and vector coupling of electron given by $a = -\frac{1}{2}$ and $v = -\frac{1}{2} + 2\sin^2\theta_W$, respectively.

3 Results

3.1 Kinematic reconstruction, event selection criteria and systematic uncertainties

The main experimental signature of CC DIS events is the presence of large transverse missing energy due to the escaped neutrino in the final state. A total of about 600 candidate events passed the selection criteria. Reconstruction of CC kinematics relies solely on

^bThe longitudinal structure function F_L is neglected in this formula.

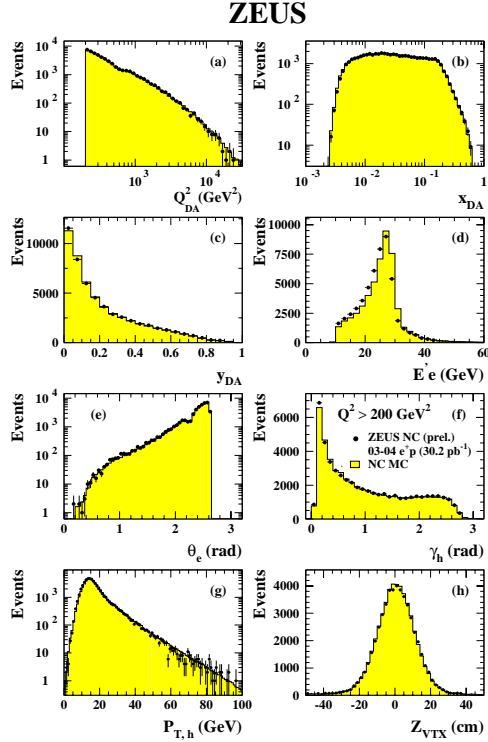


Figure 1. Comparison of NC final candidates to the Monte Carlo expectations: (a) Q^2 , (b) x , (c) y , (d) scattered electron energy, (e) scattered electron polar angle, (f) γ_h , (g) $P_{T,h}$, (h) event vertex position.

information from the recoiled hadronic system. Therefore, it is vital that the hadronic detection is well understood, which can be checked with the NC real data events.

The main experimental signature of NC DIS events is a scattered electron with a large energy. A total of about 50000 candidate events passed the selection criteria. The kinematics of NC DIS events can be reconstructed either from the scattered electron or recoiled hadronic system, or from both. This gives a good cross calibration method for example between of electro-magnetic and hadronic calorimetry. Figure 1 shows comparison of NC final candidates to the Monte Carlo (MC) expectations. It can be seen that the MC reproduces the data well, proving the validity of unfolding based on this MC in extracting the cross-sections. Also, the fact that the

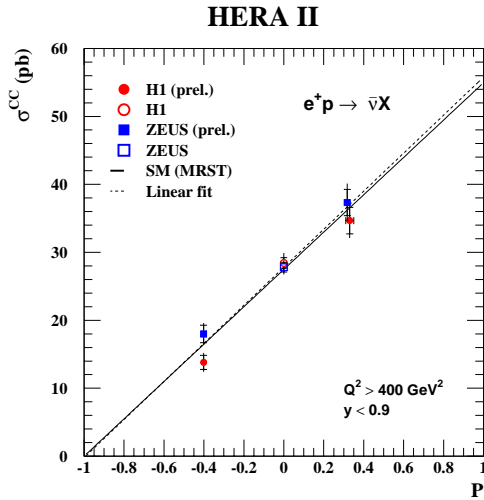


Figure 2. Charged-current total cross-section shown as a function of longitudinal polarisation of the e^+ beam.

hadronic quantities, for example the hadronic angle (γ_h) and transverse energy ($P_{T,h}$), are well described by the MC gives strong support for the CC cross section measurement.

The systematic uncertainties of the luminosity and polarisation measurements are quoted as about 2.7 (5)% and 4–6 (3)% in the H1 (ZEUS) analysis, respectively.

3.2 CC cross sections

The CC total cross-section was measured for $Q^2 > 400$ (200) GeV^2 and $y < 0.9$ (1.0) by the H1 (ZEUS) collaboration. Figure 2 shows the measured cross-sections as a function of longitudinal polarisation of the e^+ beam^c. The figure also includes the HERA-I measurements of the unpolarised CC total cross-section^{3,7}. The SM prediction with the MRST PDFs is drawn as the straight line that passes zero at polarisation $P = -1$. The measurement was consistent with the SM prediction, clearly supporting the fully parity-violating nature (i.e., $V - A$ helicity structure) of the weak charged-current inter-

^cThe ZEUS measurements were scaled to $Q^2 > 400 \text{ GeV}^2$ and $y < 0.9$.

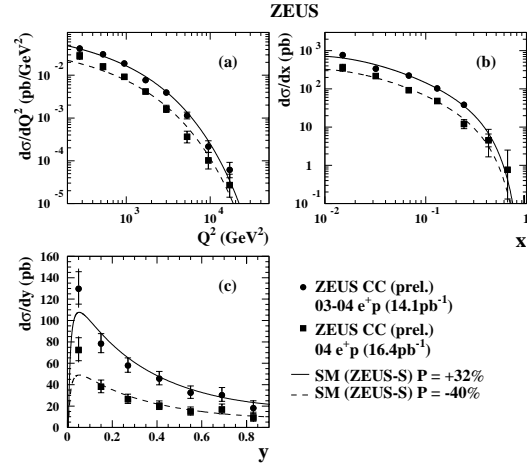


Figure 3. Charged-current differential cross-sections measured in Bjorken x , inelasticity y and four-momentum transfer squared Q^2 .

action. This is the first direct measurement showing the helicity dependence of the weak charged-current interaction at large energies. Furthermore, a linear fit was performed on the H1 and ZEUS measurements for an extrapolation of the right-handed CC cross-section, i.e., the intercept at $P = -1$. The result was:

$$\sigma_{CC}^{P=-1} = 0.2 \pm 1.8(\text{stat.}) \pm 1.6(\text{syst.})\text{pb},$$

which is consistent with the SM prediction of $\sigma_{CC}^{P=-1} = 0$. The fit result is shown in the figure as the dotted line.

In addition, the ZEUS collaboration measured single differential cross-sections in the kinematic region of $Q^2 > 200 \text{ GeV}^2$ in terms of x , y and Q^2 , respectively. As shown in Figure 3, the measurement showed a dependence of the cross-section on e^+ polarisation without any bias in kinematic phase-space, as expected from the SM.

3.3 NC cross sections

The ZEUS collaboration measured NC single differential cross-section in Q^2 at $Q^2 > 200 \text{ GeV}^2$. Figure 4 shows the measurement compared to the SM prediction with the PDFs given by the ZEUS NLO-QCD fit

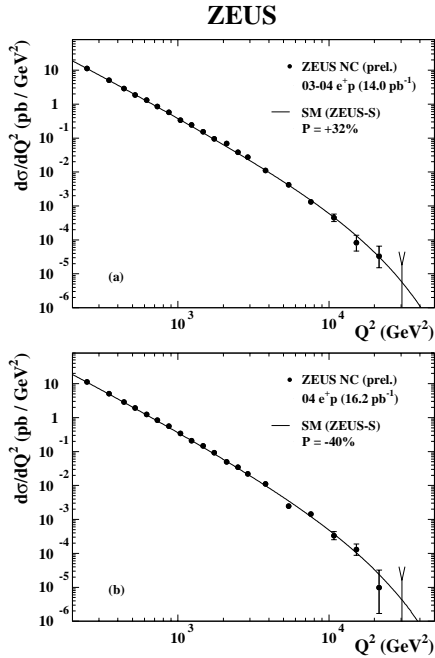


Figure 4. Neutral-current single-differential cross-section measured in four-momentum transfer squared Q^2 : for (a) positive polarisation data and for (b) negative polarisation data.

(ZEUS-S) ⁴. The measurement agrees very well with the SM prediction. Figure 5 shows the ratio of the NC cross-sections measured at $P = +32\%$ and at $P = -40\%$. The measurement is consistent with the SM prediction (shown as the dotted line in the figure), although the statistical precision of the current data set does not allow the polarised effect to be conclusively observed.

4 Summary

The cross sections for neutral and charged-current deep inelastic scattering with longitudinally polarised e^+p collisions were first measured at a luminosity-averaged positive polarisation of 33 (32)% and at a negative polarisation of about -40 (-40)% by the H1 (ZEUS) collaboration. The analysis is based on recent HERA-II runs in 2003 and 2004, which amounts to 15.3 (14.1) pb^{-1} at positive polarisation and 21.7 (16.4) pb^{-1} at negative

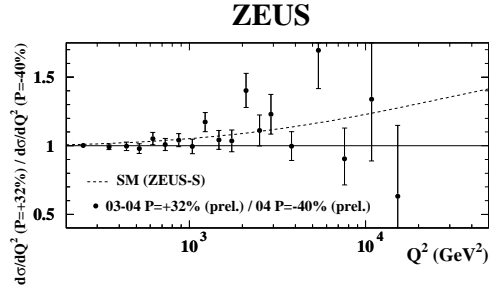


Figure 5. Ratio of the neutral-current cross-sections measured at polarisation of +32% and at polarisation of -40%.

polarisation. The measured charged-current cross section was consistent with the SM prediction, clearly supporting the fully parity-violating nature of the weak charged-current interaction as originated from the $V-A$ helicity structure. This is the first direct measurement of the helicity dependence of the weak charged-current interaction at large energies.

References

1. H1 Collaboration; C. Adloff *et.al*, *Eur. Phys. J. C* **13**, 609–639 (2000);
2. ZEUS Collaboration; S. Chekanov *et.al*, *Eur. Phys. J. C* **21**, 443–471 (2001);
3. H1 Collaboration; C. Adloff *et.al*, *Eur. Phys. J. C* **30**, 1–32 (2003);
4. ZEUS Collaboration; S. Chekanov *et.al*, *Phys. Rev. D* **67**, 012007 (2003);
5. H1 Collaboration, Contributed paper #4-0756 to this conference;
6. ZEUS Collaboration, Contributed paper #4-0256 to this conference;
7. ZEUS Collaboration; S. Chekanov *et.al*, *Eur. Phys. J. C* **32**, 1–16 (2003);
8. J. Bluemlen *et.al*, *Proc. of the HERA workshop*, 687 (1987).